AGU PUBLICATIONS

JGR

Journal of Geophysical Research: Atmospheres

RESEARCH ARTICLE
10.1002/2014JD022303

Key Points:
- Ensemble simulations to attribute O_3 response to changing emissions and climate
- Bias-correction to derive policy-relevant metrics from biased models
- Emission reductions can offset climate penalty on Eastern US surface O_3

Supporting Information:
- Text S1
- Figure S1
- Figure S2
- Figure S3
- Figure S4
- Figure S5
- Figure S6
- Figure S7
- Figure S8
- Figure S9
- Figure S10
- Table S1
- Table S2
- Table S3

Correspondence to:
H. E. Rieder,
harald.rieder@uni-graz.at

Citation:
Rieder, H. E., A. M. Fiore, L. W. Horowitz, and V. Naik (2015), Projecting policy-relevant metrics for high summertime ozone pollution events over the eastern United States due to climate and emission changes during the 21st century, *J. Geophys. Res. Atmos.*, *120*, 784–800, doi:10.1002/2014JD022303.

Received 9 JUL 2014
Accepted 5 DEC 2014
Accepted article online 9 DEC 2014
Published online 22 JAN 2015

Projecting policy-relevant metrics for high summertime ozone pollution events over the eastern United States due to climate and emission changes during the 21st century

Harald E. Rieder[1,2], Arlene M. Fiore[1,3], Larry W. Horowitz[4], and Vaishali Naik[5]

[1]Lamont-Doherty Earth Observatory, Columbia University, Palisades, New York, USA, [2]Wegener Center for Climate and Global Change and IGAM/Institute of Physics, University of Graz, Graz, Austria, [3]Department of Earth and Environmental Sciences, Columbia University, New York City, New York, USA, [4]Geophysical Fluid Dynamics Laboratory, National Oceanic and Atmospheric Administration, Princeton, New Jersey, USA, [5]UCAR, Geophysical Fluid Dynamics Laboratory, National Oceanic and Atmospheric Administration, Princeton, New Jersey, USA

Abstract Over the eastern United States (EUS), nitrogen oxides (NO_x) emission controls have led to improved air quality over the past two decades, but concerns have been raised that climate warming may offset some of these gains. Here we analyze the effect of changing emissions and climate, in isolation and combination, on EUS summertime surface ozone (O_3) over the recent past and the 21st century in an ensemble of simulations performed with the Geophysical Fluid Dynamics Laboratory CM3 chemistry-climate model. The simulated summertime EUS O_3 is biased high but captures the structure of observed changes in regional O_3 distributions following NO_x emission reductions. We introduce a statistical bias correction, which allows derivation of policy-relevant statistics by assuming a stationary mean state bias in the model, but accurate simulation of changes at each quantile of the distribution. We contrast two different 21st century scenarios: (i) representative concentration pathway (RCP) 4.5 and (ii) simulations with well-mixed greenhouse gases (WMGG) following RCP4.5 but with emissions of air pollutants and precursors held fixed at 2005 levels (RCP4.5_WMGG). We find under RCP4.5 no exceedance of maximum daily 8 hour average ozone above 75 ppb by mid-21st century, reflecting the U.S. NO_x emissions reductions projected in RCP4.5, while more than half of the EUS exceeds this level by the end of the 21st century under RCP4.5_WMGG. Further, we find a simple relationship between the changes in estimated 1 year return levels and regional NO_x emission changes, implying that our results can be generalized to estimate changes in the frequency of EUS pollution events under different regional NO_x emission scenarios.

1. Introduction

Future air quality will be affected by emissions, climate, and meteorology, thus motivating a need to better understand the drivers of future O_3 trends, and variability, including changes in high O_3 pollution events. The potential sensitivity of air pollution to climate change (e.g., recent reviews of *Fiore et al.* [2012], *Isaksen et al.* [2009], *Jacob and Winner* [2009], and *Weaver et al.* [2009]) indicates a possible "climate penalty" [e.g., *Wu et al.*, 2008] on the frequency, duration, and/or intensity of air pollution events during the course of the 21st century. We focus here on the frequency and severity (magnitude) of high-O_3 events, complementary to *Schnell et al.* [2014], who examine their duration and spatial extent.

Recent multimodel studies project regional air quality over the course of the 21st century following the representative concentration pathway scenarios (RCPs). At least three distinct modeling frameworks have been used for these future projections: (i) transient climate simulations of chemistry-climate models (CCMs) with interactive chemistry in support of the Fifth Phase of the Coupled Model Intercomparison Project (CMIP5) [*Taylor et al.*, 2012], (ii) decadal "time slice" integrations with CCMs and chemistry transport models (CTMs) in support of the Atmospheric Chemistry and Climate Model Intercomparison Project (ACCMIP) [*Lamarque et al.*, 2013], and (iii) simulations with regional CCMs or CTMs such as the Community Multi-scale Air Quality Model (CMAQ) driven by future meteorology over the U.S. [e.g., *Gao et al.*, 2013; *Pfister et al.*, 2014]. A robust feature among these model integrations is that the global NO_x decline over the 21st century

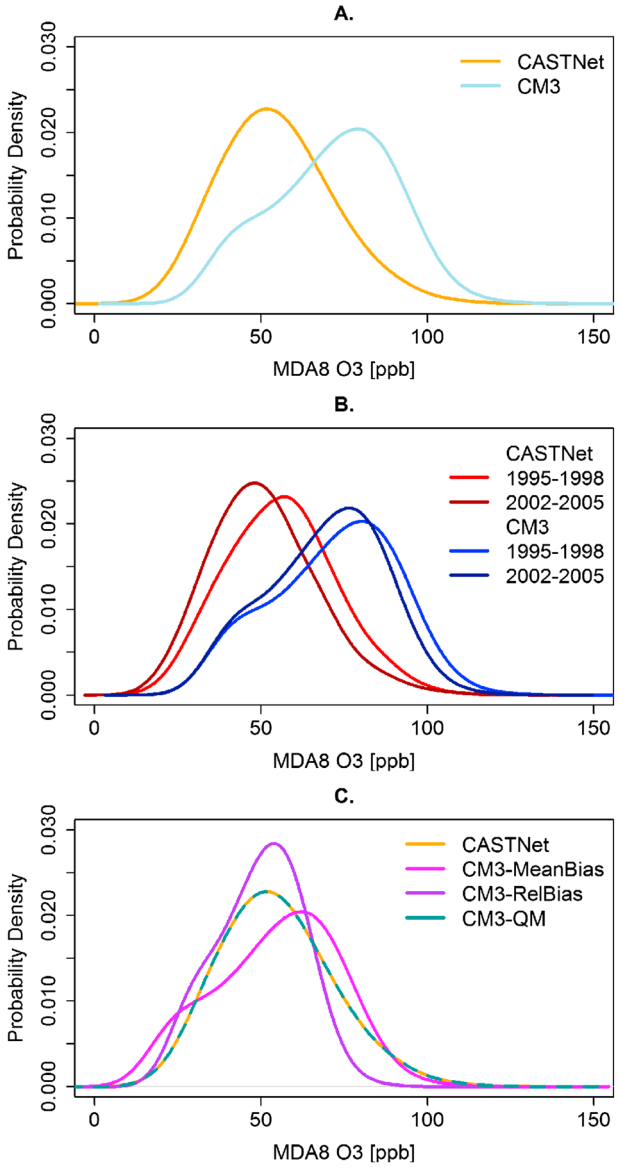

Figure 1. (a) Probability density functions of summertime (JJA) MDA8 O_3 from CASTNet and CM3 HIST (average of three ensemble members) for 1988–2005 over the eastern U.S. domain (32°N to 48°N and 68°W to 90°W). (b) Same as Figure 1a but for pre-NO_x SIP Call (1995–1998) and post-NO_x SIP Call (2002–2005) data. (c) Same as Figure 1a, but CM3 data is corrected either by subtracting the mean bias (CM3-MeanBias), relative bias (CM3-RelBias) or by the quantile mapping method (CM3-QM).

(see Figure 1 in *Fiore et al.* [2012]) leads to decreasing surface O_3 over the 21st century under all RCPs except for the RCP8.5 scenario, consistent with the projected trajectories for NO_x emissions and CH_4 abundances, suggesting that surface O_3 projections are dominated by emission changes [e.g., *Lamarque et al.*, 2011].

Although these prior modeling studies indicate decreasing mean surface ozone for the 21st century following the projected emission controls on O_3 precursors under the RCPs, several open questions remain. The large continental-scale spatial regions considered in previous multimodel analyses and the coarse resolution of the global models may mask oppositely signed changes in smaller regions, leaving open the question of how changes in emissions and climate will affect air quality at the regional scale. Furthermore, the biases of individual CCMs and CTMs compared with observations often remain unaccounted for, as the underlying physical mechanism in the model is unclear [e.g., *Parrish et al.*, 2014]. Here we address the question of how the frequency of high-ozone events will be affected by changes in regional precursor emissions and regional climate change after accounting for model ozone biases in the mean state.

Some studies have used dynamical downscaling to link global models to regional air quality models [e.g., *Avise et al.*, 2009; *Bell et al.*, 2007; *Kelly et al.*, 2012; *Weaver et al.*, 2009]. For example, *Gao et al.* [2013] use dynamical downscaling to investigate changes in maximum daily 8 hour average ozone (MDA8 O_3) for nine regions in the U.S. under present-day and future conditions. They find decreases in surface ozone pollution by the middle of the 21st century under the RCP4.5 scenario across most of the U.S. but, for the RCP8.5 scenario, note an increase in the number of days above 60 ppb, by up to 10% in the western U.S. Their analysis, however, was limited to 3 years for the 2050s from a single-model realization and did not separate out the signal from climate change versus emission changes. Recently, *Pfister et al.* [2014] applied a high horizontal resolution ensemble modeling approach to analyze changes in summertime U.S. surface ozone under the RCP8.5 scenario to show that changes in climate and global emissions of ozone precursors raise surface ozone over most of the U.S. by 2050. In contrast, they show that stringent emission controls decrease U.S. surface ozone, offsetting the increases due to the regional climate response and to the enhanced global background. The model configuration used by *Pfister et al.* [2014], however, does not separate the impacts of rising global background from regional climate warming.

Recently, we applied methods from statistical extreme value theory to maximum daily 8 h average ozone (MDA8 O_3) observed by the Clean Air Status and Trends Network (CASTNet) to quantify, in probabilistic terms, changes in both the frequency and severity of high O_3 pollution events over the eastern U.S. following the emission controls on power plants implemented through the NO_x State Implementation Plan (hereinafter, "NO_x SIP Call") [*Rieder et al.*, 2013]. We documented that the average number of summer days above the national ambient air quality standard (NAAQS) declined by about a factor of 2 from 1988–1998 to 1999–2009. Further, we described changes in eastern United States (EUS) air quality following the NO_x SIP Call in probabilistic terms, highlighting that 1 year return values of MDA8 O_3 in 1988–1999 correspond roughly to 5 year return values in 1999–2009.

Here we extend that analysis to future projections of high summertime O_3 pollution events spanning the course of the 21st century following the RCP4.5 scenario. Our approach is novel as we use (i) a bias correction method (based on quantile mapping described in section 3.1) to derive policy-relevant information at the regional scale from a biased model, using simulations and observations from the recent past; (ii) a three-member ensemble of transient simulations (section 2) to analyze the time evolution of eastern U.S. air quality out to 2100, allowing us to attribute a climate change signal distinct from internally generated model variability (noise); (iii) additional sensitivity simulations (section 2) to separate the effects of climate change alone on EUS air quality (from the full RCP4.5 scenario); and (iv) methods from statistical extreme value theory to quantify changes in probabilistic terms (sections 4.1 and 4.2). We analyze changes in the frequency of days with MDA8 O_3 above 75, 70, and 60 ppb to investigate regional exceedances of the current and potential future air quality standards over the course of the 21st century (sections 4.1 and 4.2). Finally, we relate changes in extreme events, characterized as probabilistic return levels, directly to projected changes in regional ozone precursor emissions (section 4.3), thus enabling future efforts to generalize our results to other NO_x emission scenarios.

2. Model Simulations

We analyze a suite of simulations performed with the Geophysical Fluid Dynamics Laboratory (GFDL) chemistry-climate model CM3 (hereinafter referred to as CM3) for the Coupled Model Intercomparison Project phase 5 (CMIP5) in support of the Fifth Assessment Report of the Intergovernmental Panel on Climate Change (IPCC AR5).

CM3 includes fully interactive stratospheric and tropospheric chemistry [*Austin et al.*, 2013; *Naik et al.*, 2013] and aerosol-radiation (direct and semidirect effects) and aerosol-cloud interactions (aerosol indirect effects on cloud albedo and lifetime) [*Naik et al.*, 2013]. The model applies a finite-volume dynamical core on a cubed sphere grid composed of six faces, each with a horizontal domain of 48×48 grid cells (size of an individual cell varies from 163 km at the six corners of the cubed sphere to 231 km near the center of each face) in the standard configuration, denoted as C48 horizontal resolution. CM3 includes 48 vertical hybrid sigma-pressure levels extending from the surface to 0.01 hPa (~80 km), with a 70 m thick surface layer. Tropospheric gas-phase chemistry includes reactions of NO_x-HO_x-O_x-CO-CH_4 and nonmethane volatile organic compounds based on a modified version of the chemical scheme used in the Model for OZone and Related Tracers version 2 [*Horowitz et al.*, 2003, 2007] as described by *Naik et al.* [2013].

Historical anthropogenic emissions of O_3 precursors, other than methane, in the CM3 model are from *Lamarque et al.* [2010], and those for future RCP projections are from *Lamarque et al.* [2011]. Annual-mean global-mean methane abundances from *Meinshausen et al.* [2011] are specified as a lower boundary condition in the model. Except for lightning NO_x, which is tied to the model meteorology, natural emissions of O_3 precursors are held at present-day gridded monthly mean levels from the Precursors of Ozone and their Effects in the Troposphere inventory [*Granier et al.*, 2005]. Wildfire emissions are prescribed from the ACCMIP emissions [*Lamarque et al.*, 2011; *Lamarque et al.*, 2010]. Dry deposition velocities in the model are held fixed at climatological monthly mean values, with a diel cycle imposed for ozone [*Naik et al.*, 2013]. Wet deposition is calculated interactively in the model and thus responds to simulated changes in clouds and precipitation [*Donner et al.*, 2011; *Naik et al.*, 2013]. Hourly average surface ozone fields were archived from transient simulations for both historical (HIST: 1860–2005; five ensemble members) and future (2006–2100; three ensemble members each for RCP4.5 and RCP4.5_WMGG (well-mixed greenhouse gases)) periods; we calculate the maximum daily 8 h average (MDA8) concentrations from the hourly fields.

Multiple ensemble members are used to provide a measure of the unforced internal variability ("weather noise") generated by the chaotic climate system and are generated using initial conditions separated by 50 years in the CM3 preindustrial control simulation (perpetual 1860 conditions) to launch five historical ensemble members for 1860–2005; the future simulations are then continuations from three of the respective historical ensemble members for 2006–2100.

The CM3 model and its simulations in support of CMIP5/IPCC AR5 have been extensively documented in the recent literature [e.g., *Donner et al.*, 2011; *Levy et al.*, 2013; *Naik et al.*, 2013]. Prior work relevant to this study investigated the role of emissions and climate in determining methane life time against loss by hydroxyl radical [*John et al.*, 2012], greenhouse warming-driven reductions in summertime migratory cyclones over the Great Lakes Storm Track and associated high surface O_3 events over the northeastern U.S. [*Turner et al.*, 2013], connections between the jet location and summertime surface ozone variability in the EUS [*Barnes and Fiore*, 2013], and a reversal of the surface ozone seasonal cycle over the EUS during the 21st century [*Clifton et al.*, 2014].

Here we use the CM3 simulations to study the effect of changes in emissions and climate on high surface O_3 events in the eastern U.S. We focus our analysis on the recent past (1988–2005), when data from multiple eastern U.S. sites are available for model evaluation (HIST simulation), and projections for the 21st century. We analyze results from two different future projections, in which (i) concentrations of well-mixed greenhouse gases (and stratospheric ozone-depleting substances (ODS)) and emissions of ozone precursors follow the RCP4.5 scenario and (ii) greenhouse gases follow the RCP4.5 scenario, but emissions of air pollutants and their precursors (and ODS concentrations in the chemistry scheme) are kept constant at year 2005 levels, hereinafter referred to as the RCP4.5_WMGG scenario (note that these simulations were denoted RCP4.5* in our earlier work [*Barnes and Fiore*, 2013; *John et al.*, 2012; *Turner et al.*, 2013] and that methane and ODS are treated separately in the radiation code, where they follow the RCP4.5 scenario and in the chemical mechanism, where they are held at 2005 levels). Eastern U.S. (32–48°N and 68–90°W) NO_x emissions decrease under RCP4.5 by 60% by 2030, 75% by 2050, and 84% by 2100 relative to 2005 values. We focus here explicitly on the RCP4.5 scenario as NO_x emission changes over the study region are similar among individual RCPs. NO_x emission changes in the individual RCPs by 2100 range between −84% (RCP4.5) and −95% (RCP6.0) relative to 2005 values and diverge most early in the 21st century (2020) ranging between −49% (RCP4.5) and −22% (RCP6.0) relative to 2005 values.

The analysis of multimember ensembles (five-member HIST ensemble, three-member RCP4.5, and RCP4.5_WMGG ensembles) with combined and isolated forcings represents a major advance over prior studies in the ability to detect and attribute a robust climate change signal.

3. Model Evaluation and Bias Correction

We use observations from the U.S. Environmental Protection Agency (EPA) Clean Air Status and Trends Network (CASTNet; http://www.epa.gov/castnet), which has been operating since 1987 [*Clarke et al.*, 1997]. CASTNet is representative of rural background concentrations and provides a regionally representative view of U.S. surface O_3, against which historical simulations and future projections can be assessed. Observed changes in EUS surface O_3 for CASTNet data in 1988–2009 have been described previously [*Bloomer et al.*, 2010; *Cooper et al.*, 2012; *Rieder et al.*, 2013]. Here we include CASTNet data from sites within the eastern U.S. that fulfill the following selection criteria: (i) located within the spatial domain spanning 32°N to 48°N and 68°W to 90°W, (ii) elevations greater than 2 m and less than 600 m above sea level (to avoid influence from the free troposphere) and at least 50 km inland from the oceanfront (to avoid influence of the marine boundary layer), and (iii) data coverage of at least 15 years between 1988 and 2005.

First, we compare summertime (June-July-August) MDA8 O_3 from the CM3 HIST simulations with observations from 1988 to 2005. In Figure 1a, we show the probability density functions (PDFs) of eastern U.S. MDA8 O_3 for summer in 1988–2005 for both CASTNet observations and CM3 HIST. CM3 is biased high compared to the observations (mean bias + 23 ppb; see Figure 1a and Table 1). This positive bias in eastern U.S. summertime O_3 is not unique to the CM3 model [e.g., *Fiore et al.*, 2009; *Pfister et al.*, 2014; *Rasmussen et al.*, 2012]. We note that O_3 deposition velocities are taken from the Goddard Earth Observing System–Chem model so the summertime eastern U.S. surface O_3 bias in CM3 is not affected by the problem recently identified by *Val Martin et al.* [2014].

Table 1. Station Location and Summertime (JJA) Mean Maximum Daily 8 h Average Ozone (MDA8 O_3) and the Average Number of Summer Days Above 75 ppb at EUS CASTNet Sites With the Corresponding Model Grid Cell Mean From the Uncorrected (CM3 HIST) and Corrected (CM3 $HIST_{cor}$) CM3 for 1988–2005[a]

Site Information			Mean MDA8 O_3					Average Number of Days Above 75 ppb				
-	-	-	-	-	-	Bias (model-observation)		-	-	-	Bias (model-observation)	
Station ID	Latitude (°)	Longitude (°)	Observation	CM3 HIST	CM3 $HIST_{cor}$	CM3 HIST	CM3 $HIST_{cor}$	Observation	CM3 HIST	CM3 $HIST_{cor}$	CM3 HIST	CM3 $HIST_{cor}$
ALH157	38.9	−89.6	60	78	59	18	−1	14	61	5	47	−8
ANA115	42.4	−83.9	54	73	56	19	2	9	44	10	36	2
ARE128	39.9	−77.3	62	82	63	20	1	19	66	16	47	−3
ASH135	46.6	−68.4	37	49	36	12	−1	1	5	0	4	0
BEL116[b]	39	−76.8	63	90	73	27	10	23	76	41	53	18
BVL130	40.1	−88.4	58	76	57	18	−1	11	51	5	39	−6
CDR119[b]	38.9	−80.8	51	79	60	28	9	6	61	8	55	2
CTH110	42.4	−76.7	54	67	50	13	−4	8	31	3	23	−5
ESP127[b]	36	−85.7	52	82	63	30	11	4	69	12	65	9
GAS153[b]	33.2	−84.4	55	84	65	29	10	13	67	24	54	11
LYK123	40.9	−83	58	79	61	21	3	11	58	13	47	2
MKG113	41.4	−80.1	58	81	62	23	4	14	60	17	46	3
OXF122	39.5	−84.7	60	82	63	22	3	16	68	15	53	−1
PAR107[b]	39.1	−79.7	55	82	63	27	8	7	66	16	59	9
PED108[b]	37.2	−78.3	55	85	66	30	11	6	71	24	65	18
PSU106	40.7	−77.9	58	79	61	21	3	13	57	16	44	3
SAL133	40.8	−85.7	56	79	60	23	4	10	58	11	48	1
SND152	34.3	−86	57	80	61	23	4	10	61	10	52	0
SPD111	36.5	−83.8	56	80	60	24	4	5	64	6	58	1
VIN140	38.7	−87.5	58	82	63	24	5	12	69	13	57	1
WSP144[b]	40.3	−74.9	61	88	71	27	10	21	67	38	46	17
WST109	43.9	−71.7	38	60	45	22	7	1	19	2	18	1
Mean			55	78	60	23	5	11	57	14	46	3

[a]Biases between CM3 HIST or CM3 $HIST_{cor}$ versus the CASTNet data are also given. Summary means are provided at the bottom line of the table.
[b]Indicates stations with a CM3 HIST bias versus the CASTNet observations >25 ppb.

Given the model bias and our intent to use this model to project future changes, it is important to test whether the model accurately captures the response to past emission changes. If the model response is well represented, we can apply a bias correction approach based on the present-day observed ozone distribution. This approach assumes the bias is systematic and stationary, and to the degree that this assumption holds, we can apply it to extract policy relevant information (i.e., the frequency of days above certain concentrations) from future projections made with a biased model.

The NO_x SIP Call (implemented between 1998 and 2002) provides a test case to evaluate the model response to NO_x changes. *Clifton et al.* [2014] show that CM3 captures the salient features of monthly mean changes observed at CASTNet sites over the eastern U.S. We focus here on the distribution of MDA8 O_3 in summer over this region for the pre-NO_x SIP Call (1995–1998) and post-NO_x SIP Call (2002–2005) periods, separately for both CASTNet and CM3 HIST (Figure 1b). Comparison of changes in the MDA8 O_3 PDF for pre-NO_x SIP Call and post-NO_x SIP Call indicates that CM3 largely mirrors the observed O_3 changes following an ~33% decrease in EUS NO_x emissions compared to 2000 levels [e.g., *Frost et al.*, 2006]. The CM3 pattern of changes over much of the distribution (with the exception of the low tail) is comparable to that in the observations (Figure 1b), with the strongest reductions occurring in the upper tail.

3.1. Bias Correction Method

Next we develop a bias correction, underscoring the need to continually assess the underlying processes in order to identify (and fix) the root cause of the bias and to apply process-oriented model corrections to existing simulations in future endeavors.

A common approach in model bias correction is to apply a simple correction by subtracting the mean difference between observations and model output over the entire PDF, which is commonly referred to as a mean bias correction. In Figure 1c, we show that applying such a correction improves the agreement between the CM3 HIST and CASTNet data, but significant differences remain in the upper and lower tail as

well as in the general shape of the distribution. Particularly for the high tail, which is of central interest for our study, this is problematic. Further, it should be noted that such a correction could introduce negative ozone concentrations if projected MDA8 O_3 was to fall below the mean bias. We further evaluate the application of a proportional bias correction, by subtracting the relative difference between observations and model output over the entire PDF. As found for the mean bias approach, significant differences in the shape of the distribution remain after applying the relative bias correction (Figure 1c). Therefore, we turn here to an alternative method for bias correction, which remaps the model PDF over the entire distribution to capture the overall shape and variability of the observed regional ozone distribution.

Quantile mapping (QM) is a common approach to correct biased model simulations to match observations [e.g., *Maraun*, 2013]. QM aims to establish a statistical relationship or transfer function (h) between model output (M, CM3 MDA8 O_3) and observational data (O, observed MDA8 O_3) to map the distribution (P) of the model variable onto the observed data [e.g., *Panofsky and Brier*, 1968; *Piani et al.*, 2010], see equation (1).

$$P_O = h(P_M). \tag{1}$$

To perform such mapping, we first derive maximum and minimum values as well as selected quantiles (rounded to the nearest ppb) to create a distribution q = {min, 1%, 5%, 10%, 20%, 30%, 40%, 50%, 60%, 70%, 80%, 90%, 95%, 99%, max) from both the observational (O) and the CM3 model (M) data. We derive these quantities over the joint PDFs constructed from summer ozone at 22 selected CASTNet sites from 1988 to 2005 (also used in *Rieder et al.* [2013]) and the eastern U.S. domain of CM3 HIST (excluding ocean boxes) to develop a general region-wide bias correction function for the study domain. CM3 HIST MDA8 O_3 is rounded to the nearest ppb to match the format of the CASTNet MDA8 O_3 data.

Next, we derive the differences (Δ) between the values at quantiles $q+1$ and q, individually for M (equation (2)) and O (equation (3)):

$$\Delta M_q = M_{q+1} - M_q \tag{2}$$

$$\Delta O_q = O_{q+1} - O_q. \tag{3}$$

We then calculate the ratio (R; equation (4)) between ΔO_q and ΔM_q at each quantile q

$$R_q = \frac{\Delta O_q}{\Delta M_q}. \tag{4}$$

A pointwise correction (C_j) is estimated by linearly interpolating and rescaling each model data value between two quantiles (equation (5)),

$$C_j = R_q{}^*\left(M_j - M_q\right), \text{with } M_q \le M_j < M_{q+1}. \tag{5}$$

The corrected model value at point j (M'_j) between two quantiles (equation (6)) is then calculated as

$$M'_j = O_q + C_j \tag{6}$$

leading to $P_M \neg P_O$. Since the boundaries for the correction need to be established, we set quantiles (q) and minimum and maximum of the corrected model PDF to the observed values; i.e., $q(M') = q(O)$, $\min(M') = \min(O)$, and $\max(M') = \max(O)$.

This model bias correction is applied for each ensemble member of the HIST scenario individually.

For the correction of MDA8 O_3 in the future scenarios, we derive the difference at each quantile q (equation (7)) for each raw HIST (M) and future scenario distribution ($MFUT$); pairing the future ensemble member with the HIST ensemble member from which it was launched

$$\Delta X_q = MFUT_q - M_q \tag{7}$$

and add this difference (ΔX) at quantile q to the QM-corrected HIST ensemble member (M')

$$MFUT'_q = M'_q + \Delta X_q. \tag{8}$$

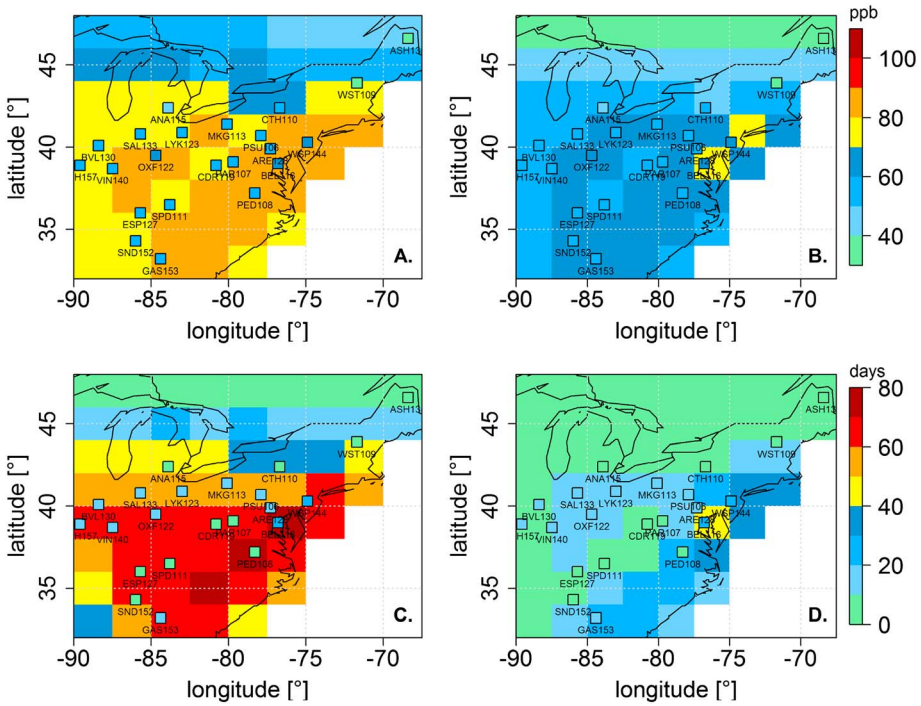

Figure 2. Maps of 1988–2005 eastern U.S. (a) mean summertime MDA8 O_3 for CM3 HIST. (b) Same as Figure 2a but for CM3 $HIST_{cor}$. (c) Average number of summer days above the NAAQS for CM3 HIST. (d) Same as Figure 2c but for CM3 $HIST_{cor}$. The squares in Figures 2a and 2b give the mean summertime MDA8 O_3 at selected CASTNet sites, while the squares in Figures 2c and 2d give the average number of summer days above 75 ppb at selected CASTNet sites.

Next we repeat equations (4)–(6) but for CM3 under each individual RCP ensemble member yielding

$$RFUT_q = \frac{\Delta MFUT'_{q+1} - \Delta MFUT'_q}{\Delta MFUT_{q+1} - \Delta MFUT_q} \tag{9}$$

$$CFUT_j = RFUT_q{}^{*}\left(MFUT_j - MFUT_q\right), \text{ with } MFUT_q \le MFUT_j < MFUT_{q+1} \tag{10}$$

$$MFUT'_j = MFUT'_q + CFUT_j. \tag{11}$$

The pointwise corrections ($CFUT_j$) are very similar (±1–2 ppb) among the individual RCP ensemble members, highlighting the robust response to changes in emissions across the CM3 ensemble members. This approach assumes that the model accurately characterizes the response to changes despite a mean state bias, as is often assumed when applying models to determine the emission controls needed to attain the NAAQS [e.g., *Simon et al.*, 2013].

3.2. Evaluation of the QM Bias Correction Method

We compare summertime regional distributions of MDA8 O_3 for the CM3 raw (HIST) and bias-corrected ($HIST_{cor}$) simulations with CASTNet data. While the uncorrected model is biased compared to the observations (as discussed above), the corrected model matches the observed regional MDA8 O_3 distribution, by design of the remapping technique (Figures 1a and 1c). We further evaluate how the regional correction approach influences the agreement between modeled and observed surface O_3 at the local scale; Figure 2 compares the summertime mean MDA8 O_3 and the average number of summer days above 75 ppb (from here on referred to as MDA8 $O_3 > 75$) as observed at the 22 selected CASTNet sites in 1988–2005 with the corrected (right) and uncorrected (left) CM3 data. We find that CM3 $HIST_{cor}$ better matches the observations (Figures 2b and 2d) at the local scale (i.e., individual sites; see also Table 1). Both the absolute magnitude and spatial pattern of the corrected model distribution (spatial correlation of MDA8 $O_3 > 75$ increases from 0.58 to 0.73), particularly in the southeastern domain (see Table 1). Threshold based statistics are particularly sensitive to biases as evident from Figure 2c, where CM3 HIST suggests that over two thirds of

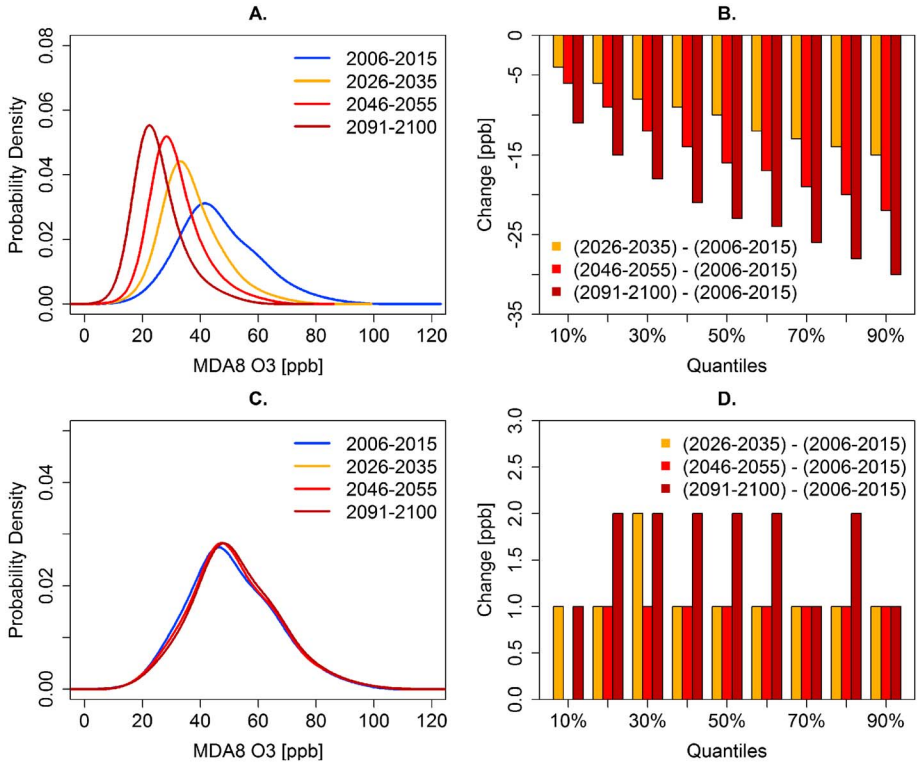

Figure 3. (a) Probability density functions of summertime (JJA) MDA8 O_3 from bias-corrected CM3 for the region in Figure 2 under the RCP4.5 scenario (average of three ensemble members) for 2006–2015 (blue), 2026–2035 (orange), 2046–2055 (red), and 2091–2100 (dark red). (b) Changes in the selected MDA8 O_3 quantiles from bias-corrected CM3 under the RCP4.5 scenario (10 to 90% quantiles in 10% steps) from a base period of 2006–2015 to 2026–2035 (orange), 2046–2055 (red), and 2091–2100 (dark red). (c and d) Same as Figures 3a and 3b but from the bias-corrected CM3 under the RCP4.5_WMGG scenario.

summer days exceed 75 ppb in some locations, while the observations indicate that this statistic is always fewer than one third of summer days.

Even for CM3 $HIST_{cor}$, local differences between individual model grid cells and the CASTNet data remain (see Figures 2b and 2d), which is expected since regional PDFs were used for the model bias correction. Although differences are small (on average 5 ppb in the mean and 3 days above 75 ppb), individual sites (those that showed a mean bias $>$ 25 ppb in CM3 HIST) still show larger deviations from the observed 1988–2005 means (up to +11 ppb), as summarized in Table 1. As a sensitivity analysis, we investigate biases in mean MDA8 O_3 and the number of days above 75 ppb in CM3 HIST and CM3 $HIST_{cor}$ relative to CASTNet data for pre-NO_x SIP Call (1995–1998) and post-NO_x SIP Call (2002–2005) periods. These comparisons show that (i) the bias-corrected CM3 data agrees with the observed statistics in both periods to within 6 ppb (mean) and within 3 days (number of days with MDA8 $>$ 75 ppb) (Tables S1 and S2 in the supporting information) and (ii) changes between the pre-NO_x SIP Call and post-NO_x SIP Call periods in the bias-corrected CM3 simulations match closely with the observations (Table S3 in the supporting information: average change in mean MDA8 O_3: CASTNet $-$6 ppb, bias-corrected CM3 $-$4 ppb; average change in the number of days above 75 ppb: CASTNet $-$5 days, bias-corrected CM3 $-$7 days). In the following sections, we analyze the projected future changes in EUS O_3 using QM-corrected CM3 distributions.

4. Projected Changes in Eastern U.S. Surface O_3 During the 21st Century

4.1. Influence of Combined Changes in Emissions and Climate

First, we focus on model simulations for the 21st century with changes in both emissions and climate under the RCP4.5 scenario. In Figure 3a, we show MDA8 O_3 distributions from the QM-corrected RCP4.5 ensemble

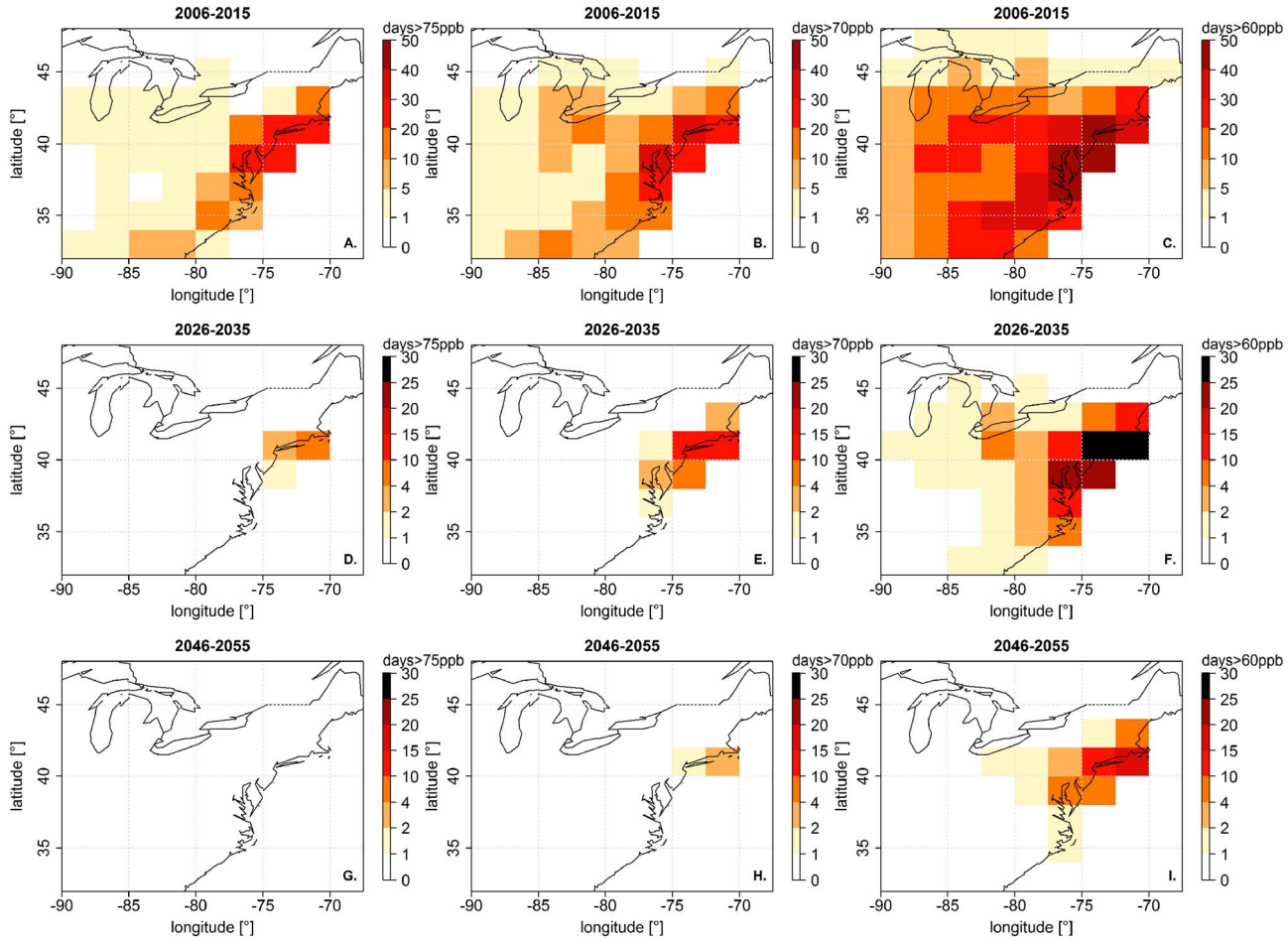

Figure 4. Average number of summer days above (a) 75 ppb, (b) 70 ppb, and (c) 60 ppb in 2006–2015. (d–f) Same as Figures 4a–4c but for 2026–2035. (g–i) Same as Figures 4a–4c but for 2046–2055. All panels show the bias-corrected CM3 simulations under the RCP4.5 scenario averaged over the three ensemble members at each grid cell.

for selected decadal periods: 2006–2015, 2026–2035, 2046–2055, and 2091–2100. Following aggressive emission controls (−60% in regional NO_x emissions projected by 2030 and −84% by 2100 relative to 2005) in the RCP4.5 scenario, the PDF of summertime MDA8 O_3 collapses as time progresses (Figure 3a). This result is consistent with the recent study of *Pfister et al.* [2014], documenting decreases in summertime surface O_3 over the U.S. under the RCP8.5 scenario.

MDA8 O_3 decreases with time over the entire distribution (reflecting the phase-in of NO_x emission controls under the RCP scenarios), with the strongest reductions occurring during the first decades (from 2006–2015 to 2026–2035). Larger changes occur in the high tail (the 90% quantile) of the distribution than in the mean (see Figure S1 in the supporting information). This finding is robust across all three ensemble members analyzed (see Figure S2 in the supporting information). The largest reductions are found spatially in regions that historically also have the highest ozone concentrations (compare CASTNet data shown in Figures 2b and 2d and Figure 3 of *Rieder et al.* [2013]).

Next we focus on statistics relevant for compliance with the NAAQS. Figure 4 shows the number of summer days with MDA8 $O_3 > 75$ through the course of the 21st century, under the RCP4.5 scenario. While several regions in the EUS exceed this level at the beginning of the 21st century (Figure 4a), the number of days with MDA8 $O_3 > 75$ declines strongly and rapidly under the RCP4.5 scenario. By 2026–2035, only 10% of the eastern U.S. model grid cells are projected to exceed 75 ppb (Figure 4d). The number of exceedances decreases with time to zero during summer by the middle of the 21st century (Figure 4g).

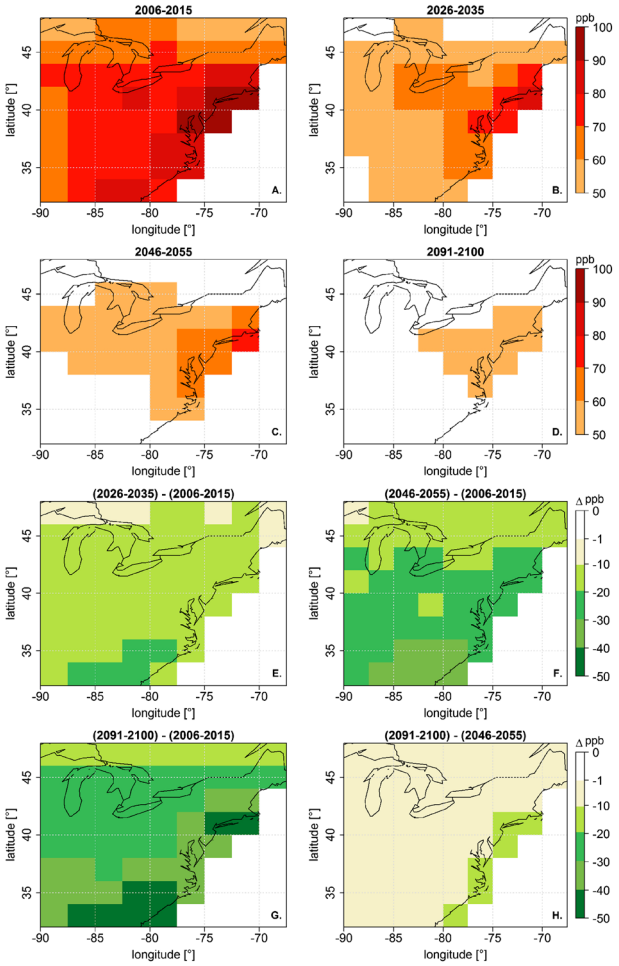

Figure 5. One year MDA8 O_3 return level estimates for (a) 2006–2015, (b) 2026–2035, (c) 2046–2055, and (d) 2091–2100. Change in the 1 year MDA8 O_3 return level from 2006–2015 to (e) 2026–2035, (f) 2046–2055, (g) 2091–2100, and (h) from 2046–2055 to 2091–2100. All panels show the bias-corrected CM3 simulations under the RCP4.5 scenario averaged over the three ensemble members at each grid cell. See section 4.1 for details. The white color over land in Figures 5a–5d indicates 1 year MDA8 O_3 return level estimates below 50 ppb.

A possible lowering of the O_3 NAAQS has been suggested [*U.S. Environmental Protection Agency* (*EPA*), 2010]. Therefore, we also evaluate in Figure 4 projections for compliance with two hypothetically lower ozone standards, representing the upper and lower end of proposed changes to the NAAQS: 70 and 60 ppb. Figure 4 also shows the average number of summer days above these levels for selected decades under the RCP4.5 scenario. Air quality improves with time following the RCP4.5 scenario, as almost no exceedance of 70 ppb is projected by the middle of the 21st century (2046–2055). For the most stringent level of 60 ppb, exceedances do occur midcentury along the northeast seaboard, but do no longer occur by the end of the 21st century (2091–2100), with the exception of one ocean grid cell south of Massachusetts (not shown). Changes in the number of summer days above 75 ppb, 70 ppb, and 60 ppb between selected decades are shown in Figure S4 in the supporting information.

In earlier work [*Rieder et al.*, 2013], we introduced a probabilistic framework based on statistical extreme value theory [e.g., *Coles*, 2001] to evaluate changes in the frequency and magnitude of high-ozone events in the EUS. Here we apply the same methodology, using a peak-over-threshold model, based on the generalized Pareto distribution (GPD), to model O_3 exceedances. The GPD ($F(x)$) is defined as

$$F(x) = 1 - \left[1 + \xi\frac{x-u}{\sigma}\right]^{-1/\xi},\ \sigma > 0,\ x > u,\ 1 + \xi\frac{x-u}{\sigma} > 0, \tag{12}$$

where x are the data (here June-July-August MDA8 O_3 from the individual QM-corrected CM3 simulations); u is the threshold (here the 90% quantile of the individual QM-corrected CM3 simulations; note that in contrast to *Rieder et al.* [2013], we are not using 75 ppb for u since maximum values in the RCP4.5 simulations drop below this value early in the 21st century); and σ and ξ are the scale and shape parameters of the GPD, fitted separately for each grid cell and decade. T-year return levels (R^T), describing the probability of exceeding a value x within a time window T, can be directly calculated from the fitted GPDs. We investigate changes in the probabilistic 1 year summertime MDA8 O_3 return level (i.e., an event of a given magnitude (level) or higher occurring once per summer (on 1 out of 92 days) over the 21st century under the RCP4.5 scenario. We focus on 1 year return levels as those estimates are constrained within narrow confidence bands.

In Figures 5a–5d, we show the 1 year return levels for the RCP4.5 scenario for selected decades during the 21st century. Under this scenario, the 1 year return levels decline strongly over the course of the 21st century, on average by 14 ppb between 2006–2015 and 2026–2035 (Figure 5e), by 18 ppb between 2006–2015 and 2046–2055 (Figure 5f) and an additional 5 ppb between 2046–2055 and 2091–2100 (Figures 5g and 5h). At the

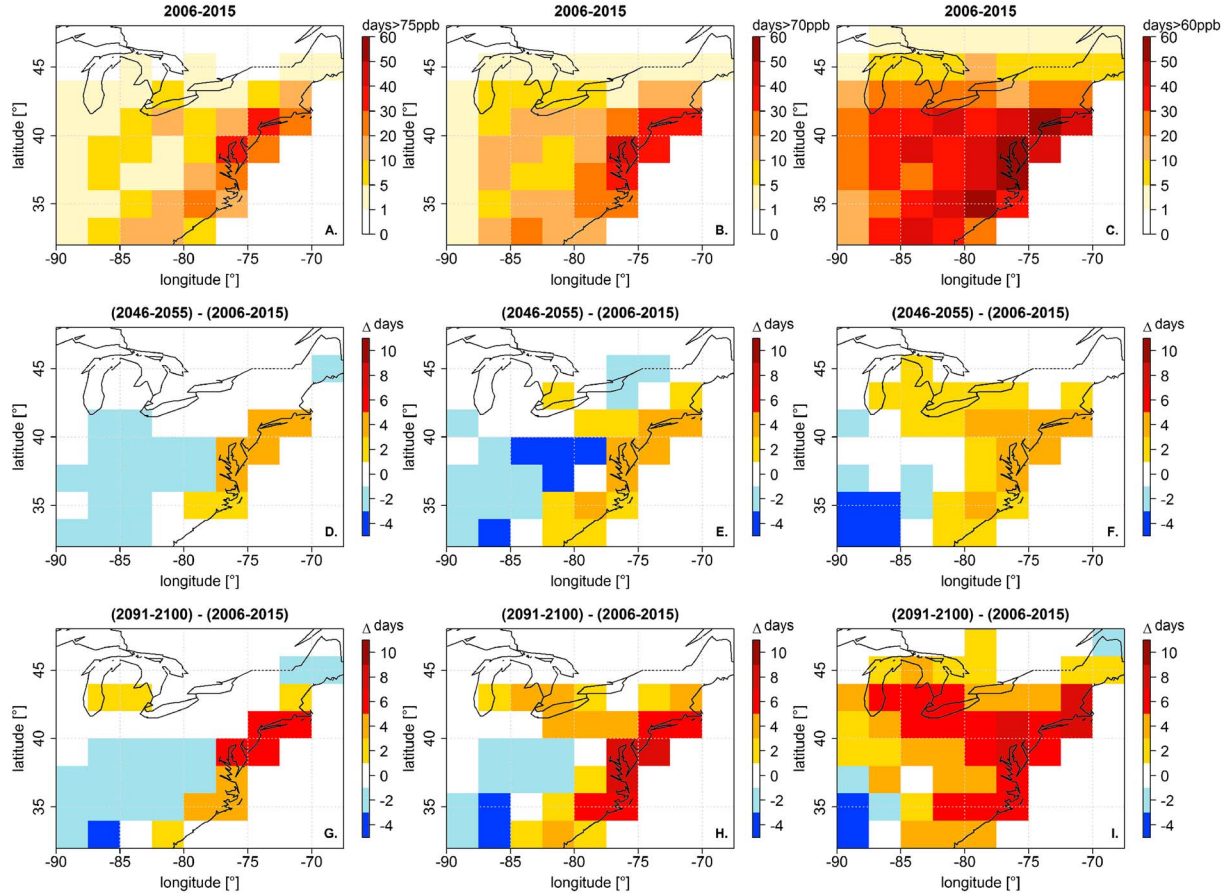

Figure 6. Average number of summer days above (a) 75 ppb, (b) 70 ppb, (c) 60 ppb in 2006–2015. Change from 2006–2015 in the average number of summer days above (d) 75 ppb, (e) 70 ppb, and (f) 60 ppb by 2046–2055. (g–i) Same as Figures 6d–6f but by 2091–2100. All panels show the bias-corrected CM3 simulations under the RCP4.5_WMGG scenario averaged over the three ensemble members at each grid cell. The average number of summer days above 75 ppb, 70 ppb, and 60 ppb by 2026–2035, 2046–2055, and 2091–2100 is shown in Figure S7 in the supporting information.

end of the 21st century, the 1 year return levels are well below 60 ppb over the entire EUS, documenting in a probabilistic framework the strong improvement in air quality and compliance with the current and possibly more stringent future air quality standards under continued emission controls.

4.2. Influence of Climate Change Alone

Now we turn to projections for the 21st century under the RCP4.5_WMGG scenario (i.e., constant emissions of ozone precursors at year 2005 levels to isolate the influence of a warming climate). The PDF of MDA8 O_3 changes little over the course of the 21st century under the RCP4.5_WMGG scenario (Figure 3c), in contrast to the RCP4.5 scenario (see Figure 3a). A closer look reveals that the PDF shifts slightly toward higher MDA8 O_3 values (by ~1 ppb by the middle and 2 ppb by the end of the 21st century), due to the effect of increased climate forcing from rising well-mixed greenhouse gases, commonly referred to as the climate penalty [e.g., *Wu et al.*, 2008]. In Figure 3d, we show changes for selected quantiles between the beginning (2006–2015; blue) and early (2026–2035; orange), middle (2046–2055; red) and end (2091–2100; dark red) of the 21st century. These results suggest, in contrast to previous work [e.g., *Weaver et al.*, 2009], that the climate penalty affects the entire MDA8 O_3 distribution in a similar way and not mainly the high tail (i.e., the extremes). This result is robust throughout the three ensemble members (see Figure S3 in the supporting information) and not influenced by the bias correction as the change at individual quantiles (ΔX_q) is by design the same for *MFUT* and *MFUT'*. We note, however, that these simulations neglect meteorologically driven feedbacks to natural emissions and deposition that might contribute to a larger response at the high tail of the O_3 distribution as noted in other modeling systems [e.g., *Leung and Gustafson*, 2005; *Nolte et al.*, 2008; *Racherla and Adams*, 2008; *Weaver et al.*, 2009; *Wu et al.*, 2008].

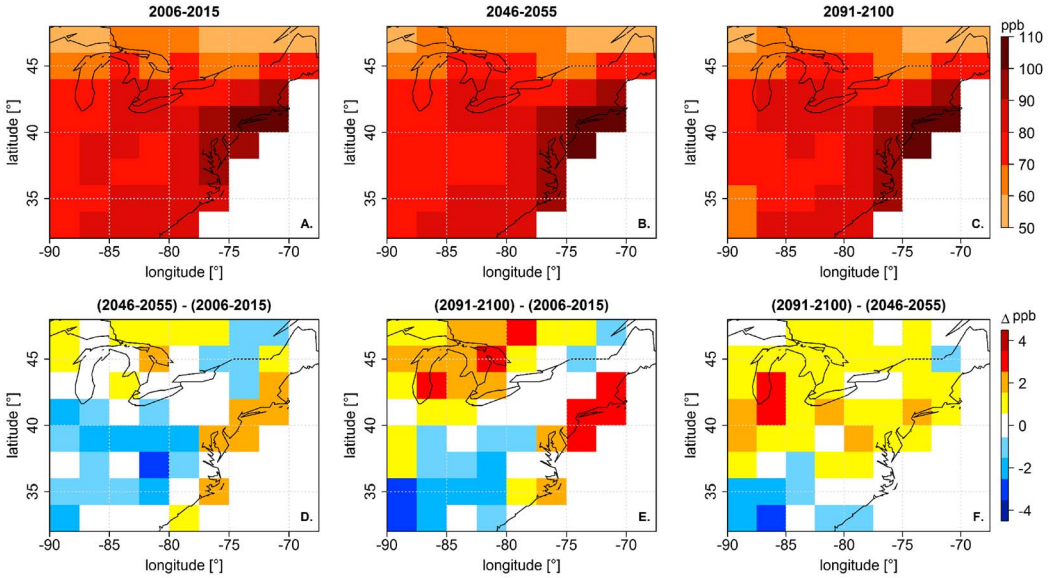

Figure 7. One year MDA8 O_3 return level estimates for (a) 2006–2015, (b) 2046–2055, and (c) 2091–2100. Change in the 1 year MDA8 O_3 return level from 2006–2015 to (d) 2046–2055, (e) 2091–2100, and (f) from 2046–2055 to 2091–2100. All panels show the bias-corrected CM3 simulations under the RCP4.5_WMGG scenario averaged over the three ensemble members at each grid cell. See section 4.1 for details.

Next we evaluate the spatial distribution of changes of mean and 90% quantile MDA8 O_3 between the beginning and middle and beginning and end of the 21st century for the RCP4.5_WMGG scenario (see Figure S5 in the supporting information). Although some decreases occur (a "climate benefit"), increases are more widespread, particularly in the Great Lakes and coastal regions. This result highlights that under a "constant emission scenario," the climate penalty from increasing well-mixed greenhouse gases would particularly affect regions that currently (2006–2015) experience the worst air quality issues (compare Figures 4 and 5 and *Weaver et al.* [2009]). MDA8 O_3 is also projected to increase at higher latitudes (i.e., the northern parts of the EUS closer to the Canadian border) under this scenario. Such changes might be related to changes in atmospheric dynamics, such as the influence of a northward shift of the jet on ozone variability, as previously documented for these simulations [*Barnes and Fiore*, 2013], and is a robust summertime feature across the current generation of climate models [e.g., *Barnes and Polvani*, 2013]. We do find some individual grid cells that show larger changes in the high tail than for the mean value, but this response is not robust across the three ensemble members or at the broader regional scale (e.g., see changes for 90th percentile versus mean values over the Great Lakes in Figure S6 in the supporting information).

We next analyze changes in the number of summer days above certain air quality levels (i.e., the current 75 ppb NAAQS and proposed lower levels of 70 ppb and 60 ppb) for the RCP4.5_WMGG scenario. Considering the 75 ppb level, we find on a decadal basis similar numbers of exceedances that increase slightly along the eastern seaboard with time (Figure 6 and Figure S7 in the supporting information), as temperatures continue to increase in response to rising well-mixed greenhouse gases (projected EUS temperature change 2006–2015 to 2091–2100 of 2.5°C). Considering the two lower possible NAAQS levels (Figure 6 and Figure S7 in the supporting information), the number of exceedances strongly increases over the course of the 21st century, reaching locally up to an additional 8 d/yr by 2091–2100.

In Figure 7, we present changes in the 1 year MDA8 O_3 return levels over the course of the 21st century under the RCP4.5_WMGG scenario. Under this scenario, a large fraction of the EUS shows 1 year return levels above 75 ppb, with nearly the entire region showing 1 year return levels above 70 ppb throughout the course of the 21st century (Figures 7a–7c). Increases in the 1 year return level are on average about 1 ppb between 2006–2015 and 2091–2100, although at the local scale (grid cell) changes of up to ±4 ppb occur in the projections (Figures 7d–7f bottom). Given the small net change, it cannot be entirely excluded that this increase in the return levels might be model noise. Inspection of the underlying individual ensemble members, however, provides confidence that the main features (increases along the eastern seaboard and

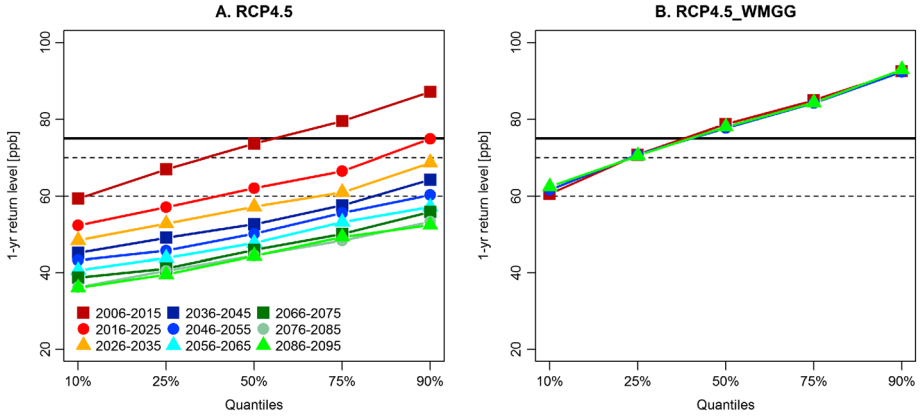

Figure 8. (a) Regional quantiles of the 1 year MDA8 O_3 return levels (i.e., fraction of individual grid cell return values averaged over the three ensemble members) on a decadal basis for the bias-corrected CM3 simulation over the EUS domain (see e.g., Figure 2) under the RCP4.5 scenario. (b) Same as Figure 8a but for the bias-corrected CM3 under the RCP4.5_WMGG scenario for 2006–2015, 2046–2055, and 2086–2095. The black solid lines in Figures 8a and 8b mark 75 ppb. The black dashed lines in Figures 8a and 8b mark lower O_3 levels of 60 and 70 ppb.

at higher latitudes and the inland, decreases over the mid-Atlantic states) are robust across the three ensemble members (see Figure S8 in the supporting information).

4.3. One Year MDA8 O_3 Return Levels and Their Response to Changing NO_x Emissions

In Figure 8, we compare the temporal evolution of regional distributions of the 1 year return level estimates for RCP4.5 and RCP4.5_WMGG. While under RCP4.5, 1 year return levels are projected to be well below 75 ppb by mid-21st century (Figure 8a), more than 50% of the EUS would experience 1 year return levels well above 75 ppb under the RCP4.5_WMGG scenario (Figure 8b). Over 90% of the eastern U.S., 1 year return levels fall

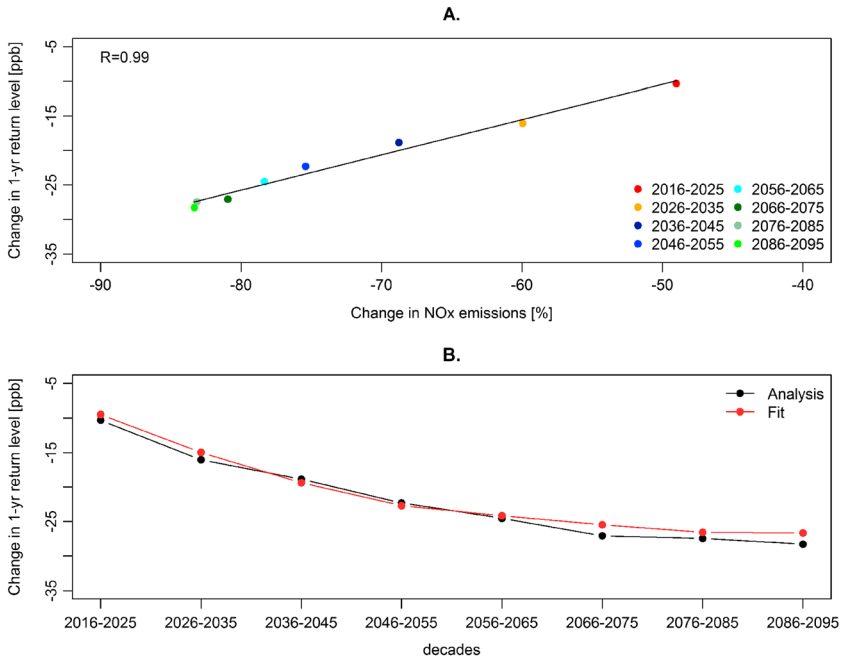

Figure 9. (a) Changes in the mean eastern U.S. 1 year MDA8 O_3 return levels as function of regional NO_x emission reductions relative to 2005, colored by decade; the correlation coefficient is reported in the top left corner of Figure 9a. (b) Comparison of the analyzed (black) and empirically fitted (red) change in the 1 year MDA8 O_3 return level on a decadal basis corresponding to eastern U.S. NO_x emission reductions relative to 2005. All panels show bias-corrected results from CM3 under the RCP4.5 scenario averaged over the three ensemble members and the eastern U.S. domain (Figure 2).

below 70 ppb by 2036–2045 and below 60 ppb by 2066–2075 under RCP4.5, while under RCP4.5_WMGG, less than 25% (70 ppb) and 10% (60 ppb) of the model grid cells are below these levels.

We find a strong relationship between changes in the 1 year return level estimates of MDA8 O_3 (ΔRL in ppb) and the regional eastern U.S. NO_x emission reductions (ΔE in percent to 2005 values) on a decadal basis during the 21st century (Figure 9a). Thus, we derive an empirical estimate for the 1 year return level changes due to emission reductions prescribed under the RCP4.5 scenario by linearly regressing the two terms:

$$\Delta\mathrm{RL} \sim C + \Delta E^{*}\beta \tag{13}$$

yielding $C = 15$ ppb and $\beta = -0.5$ ppb/% change in NO_x emission.

Applying this relationship to the projected percentage changes in regional NO_x emissions in RCP4.5 provides an estimate of changes in the 1 year MDA8 O_3 return levels for the eastern U.S. that closely matches the values projected with the full chemistry-climate model (Figure 9b). This result implies that changes in the high tail of the EUS O_3 distribution can be estimated for a wide range of NO_x emission reductions, including under moderate climate warming scenarios. For the RCP4.5 scenario, we find that a 2% reduction in regional NO_x emissions relative to 2005 yields a decline of about 1 ppb in the 1 year MDA8 O_3 return levels.

Applying the same approach to the 90% quantile and the mean of MDA O_3, we yield

$$\Delta Q90 \sim C + \Delta E^{*}\beta \tag{14}$$

with $C = 15$ ppb and $\beta = -0.5$ ppb/% change in NO_x emission, and

$$\Delta\mathrm{Mean} \sim C + \Delta E^{*}\beta \tag{15}$$

with $C = 15$ ppb and $\beta = -0.4$ ppb/% change in NO_x emission.

This result indicates a nonlinear response in MDA8 O_3 quantities to changes in regional NO_x emissions (compare Figure 3), with larger responses in the upper tail (-1 ppb/2% NO_x reduction, see Figure 9 and Figure S9 in the supporting information) then in the mean (-1 ppb/~3% NO_x reduction, see Figure S10 in the supporting information).

While other anthropogenic O_3 precursors such as carbon monoxide and volatile organic compounds are also declining under the RCP4.5 scenario, regional production of O_3 over the eastern United States in summer is well established to be in a NO_x-sensitive production regime due to the abundant availability of biogenic isoprene during summer [e.g., *Jacob et al.*, 1995; *National Research Council*, 1991]. Future analysis of additional modeling systems would enable derivation of a "best estimate" for this relationship between changes in regional anthropogenic NO_x emissions and the high tail of the O_3 distribution, in analogy to the findings of *Wild et al.* [2012] for changes in the mean state.

5. Discussion and Conclusions

We evaluated the effects of changes in ozone (O_3) precursor emissions and climate, in isolation and combination, on high summertime (June-July-August (JJA)) ozone pollution events in the eastern United States (EUS; 32°N to 48°N and 68°W to 90°W) for an ensemble of simulations performed with the Geophysical Fluid Dynamics Laboratory (GFDL) chemistry-climate model CM3.

As CM3 is biased high compared to observations available from the Clean Air Status and Trends Network (CASTNet) over the study domain, we introduce a model bias correction at the regional scale based on quantile mapping (QM) to establish a distribution from which to calculate more reliably threshold-based statistics relevant to public policy. The corrected model data agrees well with the observations (Figures 1 and 2, Table 1, and Tables S1–S3) and conserves the temporal patterns of projected changes in surface O_3 due to climate and/or emissions over the course of the 21st century.

We analyze future projections of maximum daily 8 h surface ozone (MDA8 O_3) from the QM-corrected model ($CM3_{cor}$) for summer under the representative concentration pathway (RCP) 4.5 as well as under simulations designed to isolate the impacts of climate change by holding O_3 precursor (and aerosol) emissions constant at year 2005 levels (RCP4.5_WMGG).

Under the RCP4.5 scenario, we find a strong decline in MDA8 O_3 over the entire distribution (e.g., Figures 3a and 3b). In contrast, summertime mean MDA8 O_3 increases on average by 1–2 ppb (locally by up to 4 ppb) by 2100 under the RCP4.5_WMGG scenario over the course of the 21st century (e.g., Figures 3c and 3d). In contrast to previous work [e.g., *Weaver et al.*, 2009], we find that the climate penalty due to surface warming caused by increasing atmospheric abundances of well-mixed greenhouse gases changes the entire regional O_3 probability distribution by a similar magnitude (i.e., a rightward shift) in $CM3_{cor}$ and not preferentially the high tail. However, at the local scale, i.e., within an individual model grid cell, exceptions occur, with larger changes in the high tail, but these are not generally robust across ensemble members or at the regional scale.

Next we evaluate the number of summer days exceeding the national ambient air quality standard (NAAQS, currently 75 ppb) for ozone in the eastern U.S. under both the RCP4.5 and RCP4.5_WMGG scenario. For the RCP4.5 scenario, $CM3_{cor}$ projects no exceedance of the current 75 ppb NAAQS in the eastern U.S. by the middle of the 21st century (Figure 4). In contrast under the RCP4.5_WMGG scenario, more than half of the eastern U.S. shows a significant amount of summer days (>4/year) above the NAAQS during the course of the 21st century, with the total number of days increasing by up to plus 6 days along the eastern seaboard (Figure 6).

As a lowering of the NAAQS level for ozone has been proposed [*EPA*, 2010], we also evaluate the levels of 60 and 70 ppb. Under RCP4.5, we find no exceedance of these levels by the middle (70 ppb) and end (60 ppb) of the 21st century (Figure 4). In contrast, projections under RCP4.5_WMGG show an increasing number of exceedances of these levels throughout the 21st century, reaching locally up to an additional 8 d/yr compared to 2006–2015 (Figure 6). We note that decreases also occur in some regions.

We apply a probabilistic approach (following *Rieder et al.* [2013]) to further evaluate the effect of changing emissions and climate on surface O_3; specifically, we apply methods from extreme value theory to calculate the probabilistic 1 year return levels in MDA8 O_3 within each model grid cell for the beginning, middle, and end of the 21st century under the RCP4.5 and RCP4.5_WMGG scenario. Changes in these return levels document in an illustrative way the benefit of the projected continued implementation of NO_x emission controls under the RCP4.5 scenario. While 1 year return levels are projected to decline strongly under RCP4.5, particularly during the next few decades (Figure 5), they slightly increase under the RCP4.5_WMGG scenario (Figure 7). We find that the 1 year return levels at the end of the 21st century under the RCP4.5 scenario would be well below the current NAAQS and 70 and 60 ppb levels. In contrast, under RCP4.5_WMGG, 1 year return levels are found to be well above 75 ppb throughout the 21st century over 50% of the EUS domain. This area increases to more than 75% considering a standard of 70 ppb and about 90% of the EUS under a 60 ppb standard (Figure 8). Relating changes in the eastern U.S. NO_x emissions to changes in the 1 year MDA8 O_3 return levels under RCP4.5 allows us to establish an empirical relationship between ozone precursor controls and eastern U.S. ozone return levels (Figure 9). We find that a 2% reduction in NO_x emissions relative to 2005 yields a decline of about 1 ppb in the 1 year MDA8 O_3 return levels. This simple relationship implies that our findings can be generalized to estimate changes in the 1 year return levels given different NO_x emission scenarios. Similar relationships occur for the 90% quantile and mean MDA8 O_3 (Figures S9 and S10 in the supporting information) under the RCP4.5 scenario but with a larger response to regional NO_x emission reductions in the upper tail compared to the mean of the O_3 distribution.

Overall, our results illustrate that continued regional emission controls on O_3 precursor emissions as projected under the RCP4.5 scenario would strongly improve air quality in the eastern U.S. With up to 84% decreases in regional anthropogenic NO_x emissions from 2005 levels, the CM3 chemistry-climate model indicates no exceedances of 75 ppb during the second half of the 21st century. In contrast, under present-day emissions but a moderate climate-warming scenario (RCP4.5_WMGG), surface ozone concentrations increase by an average of 1–2 ppb in the eastern U.S., reaching up to plus 4 ppb locally, by the end of the 21st century, consistent with earlier work noting a climate penalty on air pollution. We note that some regions experience a local climate benefit, up to −2 ppb. We conclude that the magnitude of the penalty or benefit from climate change is small (4–6 days decadally averaged above 75 ppb in Figure 6) compared to the roughly tenfold range of year-to-year variability in high-O_3 events, as documented from observations [e.g., *Leibensperger et al.*, 2008; *Rieder et al.*, 2013] and occurs in the model simulations analyzed here.

Acknowledgments
This article was made possible by EPA-STAR grant 83520601. Its contents are solely the responsibility of the grantee and do not necessarily represent the official view of the EPA. Further, the EPA does not endorse the purchase of any commercial products or services mentioned in the publication. H.E.R. and A.M.F. acknowledge Gustavo Correa for the computational assistance and Olivia Clifton for the MDA8 O_3 and regional temperature calculations. The authors wish to acknowledge John Dawson for the enlightening discussions. The authors are grateful to three anonymous referees for thoughtful comments on an earlier version of the manuscript. U.S. Environmental Protection Agency Clean Air Markets Division, Clean Air Status and Trends Network (CASTNet), data table accessed: Ozone 8 h Daily Max, available at www.epa.gov/castnet/, date accessed 12 July 2012. CM3 results are available upon request to the authors.

References

Austin, J., L. W. Horowitz, M. D. Schwarzkopf, R. J. Wilson, and H. Levy (2013), Stratospheric ozone and temperature simulated from the preindustrial era to the present day, *J. Clim.*, *26*(11), 3528–3543, doi:10.1175/Jcli-D-12-00162.1.

Avise, J., J. Chen, B. Lamb, C. Wiedinmyer, A. Guenther, E. Salathe, and C. Mass (2009), Attribution of projected changes in summertime U.S. ozone and PM2.5 concentrations to global changes, *Atmos. Chem. Phys.*, *9*(4), 1111–1124, doi:10.5194/acpd-8-15131-2008.

Barnes, E. A., and A. M. Fiore (2013), Surface ozone variability and the jet position: Implications for projecting future air quality, *Geophys. Res. Lett.*, *40*, 2839–2844, doi:10.1002/Grl.50411.

Barnes, E. A., and L. Polvani (2013), Response of the midlatitude jets, and of their variability, to increased greenhouse gases in the CMIP5 models, *J. Clim.*, *26*(18), 7117–7135, doi:10.1175/Jcli-D-12-00536.1.

Bell, M. L., R. Goldberg, C. Hogrefe, P. L. Kinney, K. Knowlton, B. Lynn, J. Rosenthal, C. Rosenzweig, and J. A. Patz (2007), Climate change, ambient ozone, and health in 50 U.S. cities, *Clim. Change*, *82*(1–2), 61–76, doi:10.1007/s10584-006-9166-7.

Bloomer, B. J., K. Y. Vinnikov, and R. R. Dickerson (2010), Changes in seasonal and diurnal cycles of ozone and temperature in the eastern U.S., *Atmos. Environ.*, doi:10.1016/j.atmosenv.2010.04.031.

Clarke, J. F., E. S. Edgerton, and B. E. Martin (1997), Dry deposition calculations for the clean air status and trends network, *Atmos. Environ.*, *31*(21), 3667–3678, doi:10.1016/s1352-2310(97)00141-6.

Clifton, O. E., A. M. Fiore, G. Correa, L. W. Horowitz, and V. Naik (2014), Twenty-first century reversal of the surface ozone seasonal cycle over the northeastern United States, *Geophys. Res. Lett.*, *41*, 7343–7350, doi:10.1002/2014GL061378.

Coles, S. (2001), *An Introduction to Statistical Modeling of Extreme Values*, Springer, London.

Cooper, O. R., R. S. Gao, D. Tarasick, T. Leblanc, and C. Sweeney (2012), Long-term ozone trends at rural ozone monitoring sites across the United States, 1990–2010, *J. Geophys. Res.*, *117*, D22307, doi:10.1029/2012JD018261.

Donner, L. J., et al. (2011), The dynamical core, physical parameterizations, and basic simulation characteristics of the atmospheric component AM3 of the GFDL global coupled model CM3, *J. Clim.*, *24*(13), 3484–3519, doi:10.1175/2011jcli3955.1.

U.S. Environmental Protection Agency (EPA) (2010), 75 FR 2938: National Ambient Air Quality Standards for Ozone, Proposed Rule Federal Register, pp. 2938–3052, 19 January 2010.

Fiore, A. M., et al. (2009), Multimodel estimates of intercontinental source-receptor relationships for ozone pollution, *J. Geophys. Res.*, *114*, D04301, doi:10.1029/2008JD010816.

Fiore, A. M., et al. (2012), Global air quality and climate, *Chem. Soc. Rev.*, *41*, 6663–6683, doi:10.1039/C2CS35095E.

Frost, G. J., et al. (2006), Effects of changing power plant NO_x emissions on ozone in the eastern United States: Proof of concept, *J. Geophys. Res.*, *111*, D12306, doi:10.1029/2005JD006354.

Gao, Y., J. S. Fu, J. B. Drake, J. F. Lamarque, and Y. Liu (2013), The impact of emission and climate change on ozone in the United States under representative concentration pathways (RCPs), *Atmos. Chem. Phys.*, *13*(18), 9607–9621, doi:10.5194/acp-13-9607-2013.

Granier, C., J. F. Lamarque, A. Mieville, J. F. Muller, J. Olivier, J. Orlando, J. Peters, G. Petron, G. Tyndall, and S. Wallens (2005), POET, a database of surface emissions of ozone precursors. [Available at http://www.aero.jussieu.fr/projet/ACCENT/POET.php.]

Horowitz, L. W., et al. (2003), A global simulation of tropospheric ozone and related tracers: Description and evaluation of MOZART, version 2, *J. Geophys. Res.*, *108*(D24), 4784, doi:10.1029/2002JD002853.

Horowitz, L. W., A. M. Fiore, G. P. Milly, R. C. Cohen, A. Perring, P. J. Wooldridge, P. G. Hess, L. K. Emmons, and J. F. Lamarque (2007), Observational constraints on the chemistry of isoprene nitrates over the eastern United States, *J. Geophys. Res.*, *112*, D12S08, doi:10.1029/2006JD007747.

Isaksen, I. S. A., et al. (2009), Atmospheric composition change: Climate-chemistry interactions, *Atmos. Environ.*, *43*(33), 5138–5192, doi:10.1016/j.atmosenv.2009.08.003.

Jacob, D. J., and D. A. Winner (2009), Effect of climate change on air quality, *Atmos. Environ.*, *43*(1), 51–63, doi:10.1016/j.atmosenv.2008.09.051.

Jacob, D. J., L. W. Horowitz, J. W. Munger, B. G. Heikes, R. R. Dickerson, R. S. Artz, and W. C. Keene (1995), Seasonal transition from NO_x- to hydrocarbon-limited conditions for ozone production over the eastern United States in September, *J. Geophys. Res.*, *100*(D5), 9315–9324, doi:10.1029/94JD03125.

John, J. G., A. M. Fiore, V. Naik, L. W. Horowitz, and J. P. Dunne (2012), Climate versus emission drivers of methane lifetime against loss by tropospheric OH from 1860–2100, *Atmos. Chem. Phys.*, *12*(24), 12,021–12,036, doi:10.5194/acp-12-12021-2012.

Kelly, J., P. A. Makar, and D. A. Plummer (2012), Projections of mid-century summer air-quality for North America: Effects of changes in climate and precursor emissions, *Atmos. Chem. Phys.*, *12*(12), 5367–5390, doi:10.5194/acp-12-5367-2012.

Lamarque, J. F., et al. (2010), Historical (1850–2000) gridded anthropogenic and biomass burning emissions of reactive gases and aerosols: Methodology and application, *Atmos. Chem. Phys.*, *10*(15), 7017–7039, doi:10.5194/acp-10-7017-2010.

Lamarque, J. F., G. P. Kyle, M. Meinshausen, K. Riahi, S. J. Smith, D. P. van Vuuren, A. J. Conley, and F. Vitt (2011), Global and regional evolution of short-lived radiatively active gases and aerosols in the Representative Concentration Pathways, *Clim. Change*, *109*(1–2), 191–212, doi:10.1007/s10584-011-0155-0.

Lamarque, J. F., et al. (2013), The Atmospheric Chemistry and Climate Model Intercomparison Project (ACCMIP): Overview and description of models, simulations and climate diagnostics, *Geosci. Model Dev.*, *6*(1), 179–206, doi:10.5194/gmd-6-179-2013.

Leibensperger, E. M., L. J. Mickley, and D. J. Jacob (2008), Sensitivity of U.S. air quality to mid-latitude cyclone frequency and implications of 1980–2006 climate change, *Atmos. Chem. Phys.*, *8*(23), 7075–7086, doi:10.5194/acp-8-7075-2008.

Leung, L. R., and W. I. Gustafson (2005), Potential regional climate change and implications to U.S. air quality, *Geophys. Res. Lett.*, *32*, L16711, doi:10.1029/2005GL022911.

Levy, H., L. W. Horowitz, M. D. Schwarzkopf, Y. Ming, J. C. Golaz, V. Naik, and V. Ramaswamy (2013), The roles of aerosol direct and indirect effects in past and future climate change, *J. Geophys. Res. Atmos.*, *118*, 4521–4532, doi:10.1002/jgrd.50192.

Maraun, D. (2013), Bias correction, quantile mapping, and downscaling: Revisiting the inflation issue, *J. Clim.*, *26*(6), 2137–2143, doi:10.1175/Jcli-D-12-00821.1.

Meinshausen, M., et al. (2011), The RCP greenhouse gas concentrations and their extensions from 1765 to 2300, *Clim. Change*, *109*(1–2), 213–241, doi:10.1007/s10584-011-0156-z.

Naik, V., L. W. Horowitz, A. M. Fiore, P. Ginoux, J. Q. Mao, A. M. Aghedo, and H. Levy (2013), Impact of preindustrial to present-day changes in short-lived pollutant emissions on atmospheric composition and climate forcing, *J. Geophys. Res. Atmos.*, *118*, 8086–8110, doi:10.1002/jgrd.50608.

Nolte, C. G., A. B. Gilliland, C. Hogrefe, and L. J. Mickley (2008), Linking global to regional models to assess future climate impacts on surface ozone levels in the United States, *J. Geophys. Res.*, *113*, D14307, doi:10.1029/2007JD008497.

National Research Council (1991), *Rethinking the Ozone Problem in Rural and Regional Air Pollution Rep*, 524 pp., Washington D. C.

Panofsky, H. W., and G. W. Brier (1968), *Some Applications of Statistics to Meteorology*, The Pennsylvania State Univ. Press, Philadelphia.
Parrish, D. D., et al. (2014), Long-term changes in lower tropospheric baseline ozone concentrations: Comparing chemistry-climate models and observations at northern mid-latitudes, *J. Geophys. Res. Atmos.*, *119*, 5719–5736, doi:10.1002/2013JD021435.
Pfister, G. G., S. Walters, J.-F. Lamarque, J. Fast, M. C. Barth, J. Wong, J. Done, G. Holland, and C. L. Bruyère (2014), Projections of future summertime ozone over the U.S., *J. Geophys. Res. Atmos.*, *119*, 5559–5582, doi:10.1002/2013JD020932.
Piani, C., G. P. Weedon, M. Best, S. M. Gomes, P. Viterbo, S. Hagemann, and J. O. Haerter (2010), Statistical bias correction of global simulated daily precipitation and temperature for the application of hydrological models, *J. Hydrol.*, *395*(3–4), 199–215, doi:10.1016/j.jhydrol.2010.10.024.
Racherla, P. N., and P. J. Adams (2008), The response of surface ozone to climate change over the eastern United States, *Atmos. Chem. Phys.*, *8*(4), 871–885, doi:10.5194/acp-8-871-2008.
Rasmussen, D. J., A. M. Fiore, V. Naik, L. W. Horowitz, S. J. McGinnis, and M. G. Schultz (2012), Surface ozone-temperature relationships in the eastern U.S.: A monthly climatology for evaluating chemistry-climate models, *Atmos. Environ.*, *47*, 142–153, doi:10.1016/j.atmosenv.2011.11.021.
Rieder, H. E., A. M. Fiore, L. M. Polvani, J. F. Lamarque, and Y. Fang (2013), Changes in the frequency and return level of high ozone pollution events over the eastern United States following emission controls, *Environ. Res. Lett.*, *8*(1), 014012, doi:10.1088/1748-9326/8/1/014012.
Schnell, J. L., C. D. Holmes, A. Jangam, and M. J. Prather (2014), Skill in forecasting extreme ozone pollution episodes with a global atmospheric chemistry model, *Atmos. Chem. Phys.*, *14*, 6261–6310, doi:10.5194/acpd-14-6261-2014.
Simon, H., K. R. Baker, F. Akhtar, S. L. Napelenok, N. Possiel, B. Wells, and B. Timin (2013), A direct sensitivity approach to predict hourly ozone resulting from compliance with the national ambient air quality standard, *Environ. Sci. Technol.*, *47*(5), 2304–2313, doi:10.1021/Es303674e.
Taylor, K. E., R. J. Stouffer, and G. A. Meehl (2012), An overview of CMIP5 and the experiment design, *Bull. Am. Meteorol. Soc.*, *93*(4), 485–498, doi:10.1175/Bams-D-11-00094.1.
Turner, A. J., A. Fiore, L. W. Horowitz, V. Naik, and M. Bauer (2013), Summertime cyclones over the Great Lakes Storm Track from 1860–2100: Variability, trends and association with ozone pollution, *Atmos. Chem. Phys.*, *13*, 565–578, doi:10.5194/acp-13-565-2013.
Val Martin, C., C. L. Heald, and S. R. Arnold (2014), Coupling dry deposition to vegetation phenology in the Community Earth System Model: Implication for the simulation of surface O_3, *Geophys. Res. Lett.*, *41*, 2988–2996, doi:10.1002/2014GL059651.
Weaver, C. P., et al. (2009), A preliminary synthesis of modeled climate change impacts on U.S. regional ozone concentrations, *Bull. Am. Meteorol. Soc.*, *90*(12), 1843–1863, doi:10.1175/2009bams2568.1.
Wild, O., et al. (2012), Modelling future changes in surface ozone: A parameterized approach, *Atmos. Chem. Phys.*, *12*(4), 2037–2054, doi:10.5194/acp-12-2037-2012.
Wu, S. L., L. J. Mickley, E. M. Leibensperger, D. J. Jacob, D. Rind, and D. G. Streets (2008), Effects of 2000–2050 global change on ozone air quality in the United States, *J. Geophys. Res.*, *113*, D06302, doi:10.1029/2007JD008917.